Interaction of circularly polarized pulse with solid target

Xiaomei Zhang (张晓梅), Baifei Shen (沈百飞), Yu Cang (苍 宇), Xuemei Li (李雪梅), Zhangying Jin (金张英), and Fengchao Wang (王凤超)

State Key Laboratory of High Field Laser Physics, Shanghai Institute of Optics and Fine Mechanics, Chinese Academy of Sciences, Shanghai 201800

We present the study of the interaction of an intense circularly polarized pulse with a solid target with one-dimensional (1D) particle-in-cell (PIC) simulation. The evolvement of ion motion with time is explained by a purely kinetic description and by the theory of electrostatic shock in collisionless plasmas. Especially the formation of the stable profile with a "double-flat-top" in ion phase space is explained and validated visually. Assuming the initial state, we find that the ion distribution in the phase space agrees qualitatively with the PIC simulation results by using the particle-tracing approach.

OCIS codes: 320.0320, 350.5400, 120.5700.

With the rapid development of ultrashort and ultraintense laser technology, the plasma physics emerges as a very active area of research, such as strong magnetic fields, high harmonics, fast ignition and particle acceleration. The interaction of ultraintense laser pulses with plasmas has been studied deeply and the basic mechanisms are mostly understood. With different pulse parameters and target types, the results of their interaction are different. The analytical models, for example, fluid description and kinetic description are usually used according to the given parameters. Recently, ion cascade acceleration from the interaction of a relativistic femtosecond circularly polarized laser pulse with a narrow thin solid target has been proposed by using two-dimensional (2D) particle-in-cell (PIC) simulations[1]. The formation of ion bunch induced in the interaction of circularly polarized laser pulse and overdense plasma at the front surface has been shown by using one-dimensional (1D) and 2D PIC simulations, and elucidated by a simple electrostatic and kinetic model by Macchi *et al.*[2−4]. It is a pity that there is no further explanation about the ion phase-space distribution and description about the phenomena of longer interaction time.

In this paper, we analyze the evolvement of ion motion with time from the ion-density distribution and ion-velocity distribution in phase space by 1D PIC simulation. Ions enter the undisturbed region of the target with a constant velocity and form a stable profile with a double-flat-top structure in phase space. It might be of interest for acquisition of monoenergetic ions by the present mechanism.

When a laser pulse hits the plasma, electrons are mostly pushed inwards by the laser ponderomotive force, and charge separation appears at the front surface of plasma. Then ions are accelerated by the resulting electrostatic field on a relatively longer time scale. The conditions considered in this paper is that a circularly polarized laser pulse with the wavelength of $\lambda = 1$ μm and dimensionless amplitude $a = 1$ ($a = eA/(m_e c^2)$, where A is the vector potential, c is the speed of light in vacuum and e, m_e are the electron charge and mass) illuminates an overdense plasma of initial density $n_0 = 5$, normalized by the critical density n_c for laser propagation. The target initially occupies a region from $x = 0.1\lambda$ to $x = 3.1\lambda$, where x is the propagating direction of the laser pulse. The laser field amplitude rises for $5T$ (T is the laser period) up to its maximum value and then remains constant. The ion charge and mass number are $Z = 1$ and $M = 1$, and the target is assumed to be cold. The ion mass is $m_i = 1836$, normalized by the electron mass.

When the electrostatic field is formed at the left plasma surface due to charge separation, it begins to accelerate ions. An ion bunch with high density (several times the initial value) is soon produced at the left surface of the target. The ion bunch has been also found by Macchi *et al.*. It is not in a stationary state.

In Fig. 1 we present the ion density, laser field and electrostatic field profiles at four time instants from PIC simulation. It is known that the partial ion reflection and the oscillatory velocity of transmitted ions are characteristic features of a collisionless electrostatic shock as described in Ref. [5]. However, in our simulations, all of the initially undisturbed ion (ahead of the shock front) are reflected by the large electric potential and no transmitted ion is found, so there is only single shock front structure. From ion-density distribution in Fig. 1, it is found that the right side of the bunch evolves like a shock for the density jump, but accounts for the motion of the reflected ions. A stable shock-front propagating steadily forms at the left side of the bunch about at $t = 20T$. Due to all ions reflected off the shock front, the total ion number density right side of the shock front is twice the initial density as displayed in Fig. 1.

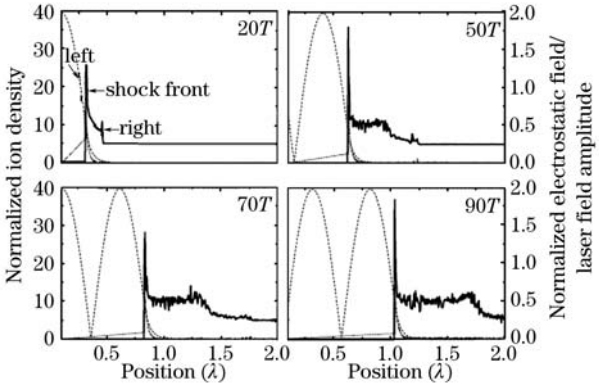

Fig. 1. Ion density n_1 (solid lines), electrostatic field (dotted lines) and laser-field amplitude a (dashed lines) at four time instants from 1D PIC simulations. A stable electrostatic shock front forms at the left side of the target.

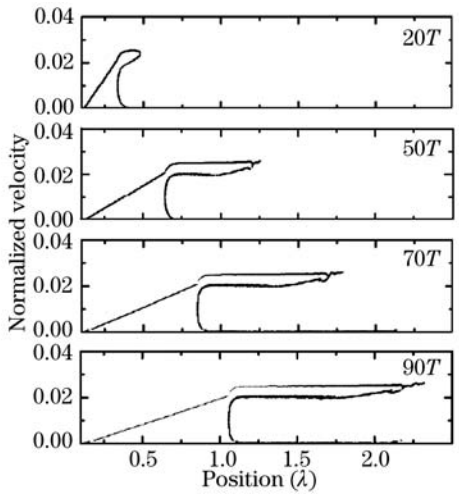

Fig. 2. Ion phase space (x, v_x) at different time for the same case as Fig. 1 profiles with double-flat-top structure are shown.

Figure 2 shows the ion-velocity distribution in phase space at the same times as in Fig. 1. The ion velocity reaches its peak and then remains constant afterward, resulting in a stable profile with a double-flat-top, as shown in Fig. 2. Ions forming the first flattop have a constant velocity of about $0.025c$ and ions forming the second flat top have a constant velocity of about $0.021c$. As shown in Fig. 1, the electrostatic field as a function of position rises up to its peak value at the surface of the plasma, and then decreases to zero. We know all ions have the constant electric potential $\varphi = 0$ before the charge separation. After ions leave the accelerative field area, they have another constant potential because the electrostatic field is zero again. Due to the energy conservation, ions have the same velocity, thus a stable profile with flat top is formed. Ions with the highest velocity are those initially located at the left of the peak value of the electrostatic field and accelerated by the whole accelerated field. Ions with relatively lower velocity are those initially located at the other side and accelerated only by the right part of the accelerative field. In fact, there are two quasi stationary states. For the first state, ions can be assumed fixed, since they have not had time to move yet due to their large mass. For the second state, ions have already caught up the electrons and have almost the same density profile as the electrons. Therefore, a double-flat-top profile in phase space forms.

From Fig. 1 and 2, we know the coordinates of the shock front structure are about $x_1 = 0.62\lambda$ at $t_1 = 50T$, and $x_3 = 1.04\lambda$ at $t_3 = 90T$, so we obtain the velocity of the shock front structure $v_\mathrm{s} = 0.0105c$ with the simple estimate

$$v_\mathrm{s} = \frac{x_2 - x_1}{t_2 - t_1}. \tag{1}$$

Because of the all ions reflected off the shock front, reflected ions have twice the shock front velocity. A model on the basis of simple momentum conservation by balancing the light pressure with the momentum flux of the inward-streaming plasma[6,7], gives the velocity of the recessing surface, and often determines the velocity of the shock, i.e.

$$2a^2 \mathrm{d}t = n_\mathrm{i} m_\mathrm{i} v_\mathrm{i} \mathrm{d}x \tag{2}$$

$$v_\mathrm{s} = \frac{\mathrm{d}x}{\mathrm{d}t} \tag{3}$$

$$v_\mathrm{i} = 2v_s \tag{4}$$

$$v_\mathrm{s} = \sqrt{\frac{1}{m_\mathrm{i}}\frac{1}{n_\mathrm{i}}}a. \tag{5}$$

In our simulation, the model predicts $v_\mathrm{s} = 0.0104c$, corresponding to the velocity $v_\mathrm{i} = 2v_\mathrm{s} = 0.0208c$ of reflected ions, in good agreement with the relatively lower velocity observed in our simulation.

Figure 3 gives the ion phase space distribution at two instants at later time. Most ions initially at the left of the electrostatic field peak will be dragged into the right side and ion density in the first flat top in ion phase space becomes very small, while the ions initially in front of the shock front are accelerated continually to form the second flat top. The ions at the rear of the target $(x > 3.1\lambda)$ are also accelerated a little by expansion into vacuum.

A new purely kinetic model for this ion phase-space distribution is presented. For ions, they are driven only by electrostatic force, and then the key problem is how to obtain the electrostatic field. Assuming the initial state is the equilibrium state for electrons with the electrostatic force balancing the ponderomotive force, while ions is supposed to be fixed due to their slow response to the electrostatic field at that time, we start with the Maxwell's equations for the electromagnetic field and the relativistic equation of motion for electrons. With boundary conditions, the expression of the electrostatic field is

$$E_x = -\frac{\partial \phi}{\partial x} = (\gamma - 1)\left[(\gamma + 1)(2n_0 - \gamma - 1)\right]^{1/2}, \tag{6}$$

which is also obtained in Refs. [8] and [9], where $\phi = e\varphi/(m_\mathrm{e}c^2)$ is the normalized electric potential and $\gamma = \sqrt{1 + a^2}$ is the relativistic factor. Figure 4 shows the distributions of the electrostatic field and potential calculated from Eq. (6). The electrostatic field rises up to a maximum value and then decreases to zero, and it is only related to the initial density and intensity of incident light. The electric potential increases to a constant value $\phi = -0.56$ from zero. According to the energy conservation

$$\phi + \frac{1}{2} m_\mathrm{i} v_\mathrm{i}^2 = 0, \tag{7}$$

the velocity of ions initially located at the left of the peak

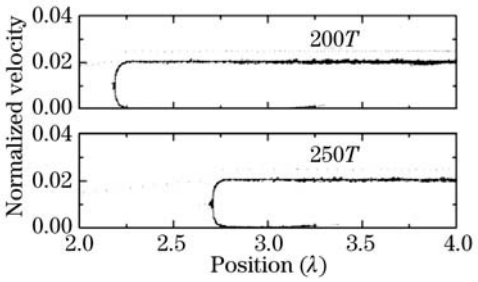

Fig. 3. Ion phase space at $t = 200T$ and $250T$ for the same case as Fig. 1. The first flat top tends to disappear.

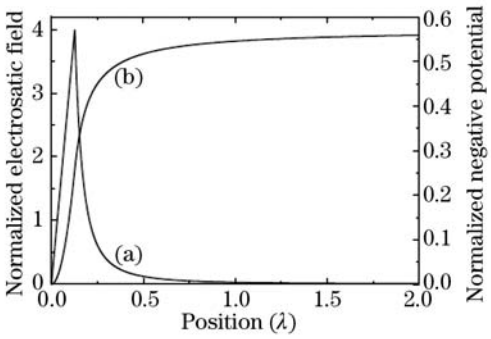

Fig. 4. Electrostatic field E_x (a) and negative potential (b) of equilibrium state for the same case as before.

value of the electrostatic field is about $0.0246c$, in good agreement with the first flat-top velocity observed in Fig. 2.

By using the particle-tracing approach and the Newton's equation of motion, we get the ion-velocity distribution in the phase space at different times, as shown in Fig. 5, which agrees qualitatively with the PIC simulations. Ions to the right of the maximum value of the electrostatic field move slower than others and would be caught up by the ions moving faster beyond them. So there is a curve in the phase-space distribution. Additionally, difference exists between the simulation and analytical results, because the ions in our assumed equilibrium state have different electric potentials, and the equilibrium state is not a stationary state. As shown in Fig. 1, the electrostatic field changes with time and moves together with target, while we assume it remains constant. Anyway, the analytical results verify our explanation.

The ponderomotive forces on electrons are different for different polarization states. For linearly polarized pulses, much theoretical and experimental work has been devoted. The ponderomotive force contains both time-independent and time-dependent components[10]. Hot electrons can be generated by the time-dependent component with double frequency of the incident laser pulse[11]. They are required for ion acceleration whether the ions are mainly accelerated by the rear sheath acceleration[12−14] model or front-shock acceleration[6,15]

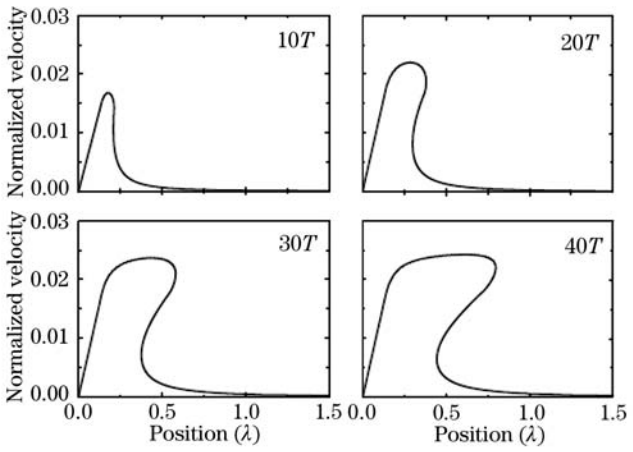

Fig. 5. Ion phase space of the analytical results at different times. The cases studied are the same as in Fig. 1.

model. Because of the propagation of hot electrons, most ions are influenced quickly, and the density profile is turbulent[2,16].

It has been shown that, for linearly polarized laser pulses, ions are first accelerated by the electrostatic field induced by the charge separation at the front surface, with a phenomenon called "hole-boring"[17]. The time-dependent component of ponderomotive force oscillates with electrons strongly in the longitudinal direction and simultaneously excites an electrostatic wave with double frequency of the incident laser pulse. Subsequently, an ion wave is launched and then evolved into a shock, and ions are reflected at twice the shock velocity. However, for circularly polarized pulses, it is well known that the time-dependent component of the ponderomotive force is zero for its symmetry and there is only the steady component, i.e. light pressure, and no hot electron is generated by the time-dependent component. Microscopically, ions already have been accelerated to twice the shock velocity by the electrostatic field induced by charge separation. However, it looks like that ions are reflected off the shock front macroscopically.

The important question of the ion bunch and shock formation in two and three dimensions is beyond the scope of the present paper. Both the PIC simulation and analytical model here are in 1D case, and are expected to be valid if the focusing area is sufficiently large.

In conclusion, the interaction of a circularly polarized pulse with a cold solid target is studied. A profile with double-flat-top in ion phase space is found from 1D PIC simulation. The stable shock front structure near the laser reflection surface is formed after a relatively long time. With the particle-tracing approach we find that the ion distribution in the phase space agrees qualitatively with the above PIC simulations. We hope the results can shed light on the interaction of a circularly polarized femtosecond laser pulse and a thin solid target.

This work was supported by the National Natural Science Foundation of China under Grant No. 10675155. X. Zhang's e-mail address is zhxm@siom.ac.cn.

References

1. F. He, H. Xu, Y. Tian, W. Yu, P. Lu, and R. Li, Phys. Plasmas **13,** 073102 (2006).
2. A. Macchi, F. Cattani, T. V. Liseykina, and F. Cornolti, Phys. Rev. Lett. **94,** 165003 (2005).
3. A. Macchi, F. Cattani, T. V. Liseykina, and F. Cornolti, *CP827,* in *Superstrong Fields in Plasmas: Third International Conference on Superstrong Fields in Plasmas* 215 (2006).
4. T. V. Liseykina, A. Macchi, F. Cattani, and F. Cornolti, in *32nd EPS Conference on Plasma Phys. Tarragona* **29C,** 4.149 (2005).
5. D. A. Tidman and N. A. Krall, *Shock Waves in Collisionless Plasmas* (Wiley-Interscience, New York, 1971).
6. L. O. Silva, M. Marti, J. R. Davis, and R. A. Fonseca, Phys. Rev. Lett. **92,** 015002 (2004).
7. W. Yu, M. Yu, J. Zhang, and Z. Xu, Phys. Rev. E **58,** 6553 (1998).
8. W. Yu, M. Yu, Z. Sheng, and J. Zhang, Phys. Rev. E **58,** 2456 (1998).
9. B. Shen and J. Meyer-ter-vehn, Phys. Plasmas **8,** 1003

(2001).

10. S. Liu, Q. Tu, W. Yu, Z. Chen, and J. Zhang, Chin. Phys. Lett. **18,** 646 (2001).
11. S. C. Wilks, W. L. Kruer, M. Tabak, and A. B. Langdon, Phys. Rev. Lett. **69,** 1383 (1992).
12. S. Betti, F. Ceccherini, F. Cornolti, and F. Pegoraro, Plasma Phys. Control Fusion **47,** 521 (2005).
13. Q. Dong, Z. Sheng, M. Yu, and J. Zhang, Phys. Rev. E **68,** 026408 (2003).
14. P. Mora, Phys. Rev. Lett. **90,** 185002 (2003).
15. M. S. Wei, S. P. D. Mangles, Z. Najmudin, B. Walton, A. Gopal, M. Tatarakis, A. E. Dangor, E. L. Clark, R. G. Evans, S. Fritzler, R. J. Clarke, C. Hernandez-Gomez, D. Neely, W. Mori, M. Tzoufras, and K. Krushelnick, Phys. Rev. Lett. **93,** 155003 (2004).
16. J. Denavit, Phys. Rev. Lett. **69,** 3052 (1992).
17. E. d'Humières, E. Lefebvre, L. Gremillet, and V. Malka, Phys. Plasmas **12,** 062704 (2005).